ADVANCES IN ATMOSPHERIC SCIENCES, VOL. 31, JULY 2014, 879–887

Retrieval of Aerosol Optical Properties over a Vegetation Surface Using Multi-angular, Multi-spectral, and Polarized Data

WANG Han*[1,2,3], SUN Xiaobing[1,2], SUN Bin[1,2,3], LIANG Tianquan[1,2,3], LI Cuili[1,2,3], and HONG Jin[1,2]

[1]*Anhui Institute of Optics and Fine Mechanics, Chinese Academy of Sciences, Hefei* 230031
[2]*Key Laboratory of Optical Calibration and Characterization, Chinese Academy of Sciences, Hefei* 230031
[3]*University of Chinese Academy of Sciences, Beijing* 100049

(Received 13 May 2013; revised 22 September 2013; accepted 12 November 2013)

ABSTRACT

An algorithm to retrieve aerosol optical properties using multi-angular, multi-spectral, and polarized data without a priori knowledge of the land surface was developed. In the algorithm, the surface polarized reflectance was estimated by eliminating the atmospheric scattering from measured polarized reflectance at 1640 nm. A lookup table (LUT) and an iterative method were adopted in the algorithm to retrieve the aerosol optical thickness (AOT, at 665 nm) and the Ångström exponent (computed between the AOTs at 665 and 865 nm). Experiments were performed in Tianjin to verify the algorithm. Data were provided by a newly developed airborne instrument, the Advanced Atmosphere Multi-angle Polarization Radiometer (AMPR). The AMPR measurements over the target field agreed well with the nearby ground-based sun photometer. An algorithm based on Research Scanning Polarimeter (RSP) measurements was introduced to validate the observational measurements along a flight path over Tianjin. The retrievals were consistent between the two algorithms. The AMPR algorithm shows potential in retrieving aerosol optical properties over a vegetation surface.

Key words: multi-angle, multi-spectra, polarization measurement, aerosol optical properties, AMPR

Citation: Wang, H., X. B. Sun, B. Sun, T. Q. Liang, C. L. Li, and J. Hong, 2014: Retrieval of aerosol optical properties over a vegetation surface using multi-angular, multi-spectral, and polarized data. *Adv. Atmos. Sci.*, **31**(4), 879–887, doi: 10.1007/s00376-013-3100-5.

1. Introduction

Climate (Duan et al., 2012; Hansen et al., 1998) and environment (Brunekreef and Holgate, 2002) are affected by aerosols because they change the energy cycle (Haywood and Boucher, 2000). The quantity of aerosol is an important parameter. However, the large spatial and temporal variability of aerosol properties (Dai et al., 2014) make assessing the effect of aerosol particles on the local air quality and global climate difficult. Though scientists have made many attempts to quantify aerosol properties, remote sensing is one of the most useful methods to date.

Satellite remote sensing is a significant way to detect global aerosol optical properties (Diner et al., 2005; Hauser et al., 2005; Remer et al., 2005). The upwelling total radiance which is used to derive the aerosol optical properties includes atmospheric reflectance, land surface reflectance, and the surface–atmosphere interactions (Waquet et al., 2009a). All three parts need to be separated from the total reflectance, since each part is the function of various parameters. Accurate estimation of the land surface and aerosol reflectance is important in aerosol retrieval as it is a challenging problem for intensity measurement. However, it can be better solved by using a polarization measurement. Lower relative contribution, less spectral dependence, and less spatial contrast are three obvious advantages of using a polarization measurement to estimate the surface contribution (Deuzé et al., 1993; Waquet et al., 2007, 2009b). Moreover, many experimental and theoretical studies have shown that polarization measurements exhibit a higher sensitivity to aerosol properties than to land surface (Mishchenko and Travis, 1997; Cairns et al., 1997; Chowdhary et al., 2005).

Taking advantage of these features of polarization, Deuzé et al. (2001) developed a method based on polarized radiance measurements to retrieve the aerosol optical thickness over lands at 670 and 865 nm with an a priori knowledge of the land surface. The measurements were provided by the Polarization and Directionality of the Earth Reflectance instruments (POLDER). Combined polarization and intensity measurements were used to retrieve ocean aerosol properties from Polarization and Anisotropy of Reflectances for Atmospheric Sciences Coupled with Observations from Lidar (PARASOL) multi-angle photopolarimetric measurements (Hasekamp et al., 2011) which improved the agreement with the Aerosol Robotic Network (AERONET) retrievals com-

* Corresponding author: WANG Han
Email: ms.h.wang@163.com

pared to intensity-only retrievals. A general applied method has been developed by Dubovik et al. (2011) in which both the aerosol and surface models are used to simulate total and polarized reflectance. It can be used to retrieve aerosol and surface properties simultaneously from multi-spectral and multi-angular data and is derived from POLDER measurements. Before obtaining satellite observations, airborne measurements are essential to develop and improve the retrieval algorithms. Airborne simulators based on the Research Scanning Polarimeter (RSP) (Cairns et al., 1997; Chowdhary et al., 2002; Cairns et al., 2003; Waquet et al., 2009b) and the microPOL (Waquet et al., 2005, 2007) have been developed. The RSP provides multi-angular, multi-spectral, and polarized data. Measurements at 2250 nm are used to estimate the land surface polarized reflectance, and the aerosol optical properties are retrieved using an optimal estimation method (Waquet et al., 2009a). Knobelspiesse et al. (2008) introduced an iterative method to solve the diffuse and multiple interaction terms and the kernel values of the Ross–Li surface reflectance model using RSP data. MICROPOL is a single viewing and multi-spectral prototype polarimeter that provides accurate polarized measurements in five spectral bands. The accuracy and stability of retrieval algorithms associated with the single view angle operation of MICROPOL are limited by assuming aerosol microphysical models. In China, Cheng et al. (2011) used a Directional Polarimetric Camera (DPC) to retrieve aerosol optical properties over cities. A DPC detects the same target twice, at 200 m and 4000 m to estimate the land surface and atmosphere, respectively. However, more monitoring is needed over the vast regions in China.

To better monitor aerosols in China, the Anhui Institute of Optics and Fine Mechanics, Chinese Academy of Science (AIOFM-CAS) has developed the Advanced Atmosphere Multi-angle Polarization Radiometer (AMPR) with high polarized detection accuracy. It can obtain multi-angular, multi-spectral and polarized data. A more detailed discussion of the AMPR is found in section 2.

This paper focuses on the retrieval algorithm of aerosol properties using multi-angular, multi-spectral, and polarized data from the AMPR over vegetation without a priori knowledge of land surface. We introduced an iterative method to quantify the polarized reflectance of the land surface and aerosol. The polarized reflectance at 1640 nm was selected as the initial estimate of surface. Then, an iterative method was adopted to obtain the reflectance of the land surface and atmosphere step by step. Retrievals of the ground-based sun photometer (CE318) were used to validate the algorithm (Dubovik and King, 2000; Li et al., 2006). The algorithm, based on RSP measurements (RSP algorithm) and developed by Waquet et al. (2009a), was also used for the validation of the AMPR algorithm.

2. Instrument, calibration and data selection

The AMPR sensor is currently a sub-orbital based prototype that will eventually become space-based. The main goal of the AMPR is to retrieve a suite of aerosol and cloud optical thicknesses and parameters over land. The spectral and spatial responses of radiance measurements are complex, so the AMPR has six polarized spectral channels with center wavelengths at 490, 555, 665, 865, 960, and 1640 nm. Measurements at 665, 865, and 1640 nm were used to retrieve aerosol properties in this paper where the molecular and aerosol optical thicknesses were small. Accordingly, the multiple scattering influences were less and the single scattering approximation is realistic (Bréon et al., 1997). The 960 nm measurements were used to estimate the water vapor column amounts.

The AMPR scan starts from -55° to $+55^\circ$ of nadir with a sampling interval of 1°. Thus, each scan contains 111 instantaneous samples at every wavelength. Two Wollaston prisms were used to detect the polarization in the 0°, 90°, 45°, and 135° directions. The subastral point spatial resolution was about 52 m at an altitude of 3 km with a scan period of 0.8630 s. About one-third of the time was used to scan the target and the remaining time was reserved for calibration purposes.

Calibration of the AMPR was based on Song et al. (2012) in order to eliminate the instrumental polarization effects and to derive the calibrated polarization parameters. Before and after the flight experiment, the AMPR was calibrated twice in the laboratory. There were 15 days between these two calibrations. The accuracy of the degree of linear polarization (DoLP) was better than 0.01. The calibration lamp attached to the AMPR instrument functioned while measurements were being taken. Data show that the AMPR was in normal operating conditions.

The measured polarized reflectance of a scan period was the input of the algorithm. The relative polarized radiance of the vegetation surface had less spectral dependence (Waquet et al., 2007, 2009b). All three wavelengths shared the same surface polarized reflectance. We assumed that the atmospheric conditions did not change during the scanning period. Hence, we can obtain the multi-angular scattering information of aerosol. When the scattering angle was larger than 160°, the spectral responses of polarized reflectance were negligible and thus, the data were omitted.

3. Aerosol retrieval algorithm of AMPR

3.1. *Polarized reflectance at viewing level*

The normalized total radiance, R, and normalized polarized radiance, R_p, are defined from Stokes' vector:

$$R = \frac{\pi I}{\mu_\mathrm{s} E_0}\,, \tag{1}$$

$$R_\mathrm{p} = \frac{\pi\sqrt{Q^2+U^2}}{\mu_\mathrm{s} E_0}\,, \tag{2}$$

where E_0 is the flux density at the top of atmosphere and μ_s is the cosine of the solar zenith angle. Thus, the upward polarized reflectance at the viewing altitude can be simulated in

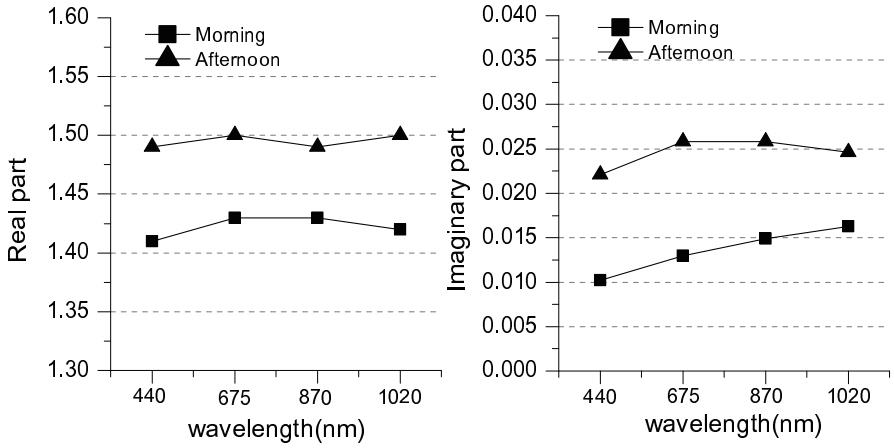

Fig. 1. Complex refractive index of aerosol at the moment of plane transit on 10 August 2012 over target field (TF).

the following form (Cairns et al., 1997; Deuzé et al., 2001):

$$R_{\mathrm{p,simu}}(\lambda,\theta_{\mathrm{s}},\theta_{\mathrm{v}},\varphi,a) = R_{\mathrm{p,atmo}}(\lambda,\theta_{\mathrm{s}},\theta_{\mathrm{v}},\varphi,a) + T_1(\lambda,\theta_{\mathrm{s}},\theta_{\mathrm{v}},\varphi,a)R_{\mathrm{p,surf}}(\theta_{\mathrm{s}},\theta_{\mathrm{v}},\varphi)T_2(\lambda,\theta_{\mathrm{s}},\theta_{\mathrm{v}},\varphi,a)\ , \quad (3)$$

where θ_{v} is the viewing zenith angle, θ_{s} is the solar zenith angle, and φ is the relative azimuth angle. λ is the wavelength. The letter "*a*" represents the atmospheric optical properties, which include the molecular and aerosol optical properties. $R_{\mathrm{p,atmo}}$ is the contribution of the atmosphere polarized reflectance and $R_{\mathrm{p,surf}}$ is the bidirectional polarized reflectance factor. T_1 and T_2 are the downward and upward transmission terms, respectively:

$$T_1 = \exp\left[-\left(\frac{\psi\tau_{\mathrm{mole}} + \varsigma\tau_{\mathrm{aero}}}{\mu_{\mathrm{s}}}\right)\right]\ , \quad (4)$$

$$T_2 = \exp\left\{-\left[\frac{\psi\tau_{\mathrm{mole}}(z) + \varsigma\tau_{\mathrm{aero}}(z)}{\mu_{\mathrm{v}}}\right]\right\}\ . \quad (5)$$

Here, ψ and ς are estimated by Lafrance (1997), z is the viewing altitude and μ_{v} is the cosine of the viewing zenith angle. The molecule and aerosol optical thickness below level z can be calculated as

$$\tau_{\mathrm{mole}}(z) = [1-\exp(-z/H_{\mathrm{m}})]\tau_{\mathrm{mole}}\ , \quad (6)$$

$$\tau_{\mathrm{aero}}(z) = [1-\exp(-z/H_{\mathrm{a}})]\tau_{\mathrm{aero}}\ , \quad (7)$$

where τ_{mole} and τ_{aero} are the whole optical thicknesses of the molecule and aerosol, respectively. H_{a} and H_{m} are set to approximately 2 km and 8 km, respectively (Waquet et al., 2007, 2009b).

3.2. *Aerosol retrieval scheme*

We report the results of the CE318 retrievals on 10 August 2012. These results demonstrate the temporal variability of the aerosol optical properties over the target field. Figure 1 shows the complex refractive index of the aerosols at the moment of plane transit, including the real and imaginary parts. Both the real and imaginary parts are nearly steady at the different wavelengths but change after a period of time. Figure 2 shows the size distribution of the aerosols at the same time with the refractive index. The amount of small aerosol particles decreased and the center of the first peak moved left in the afternoon. As polarization is more sensitive to small particles than large ones (Deuzé et al., 2001), these changes are reflected by the aerosol optical thickness (AOT) and the Ångström exponent. The aerosol distribution is time-varying and is considered in the retrieval.

A lookup table (LUT) approach was adopted in the algorithm to retrieve the AOT and the Ångström exponent. The Ångström exponent was introduced as an incarnation of the aerosol size distribution and the refractive index. Low Ångström exponent values correspond to large particles, while large values correspond to small particles, as the Ångström exponent is a function of the size distribution and refractive index. The aerosol scattering phase function is related to these two parameters as well and is therefore related to the Ångström exponent. The Ångström exponent is

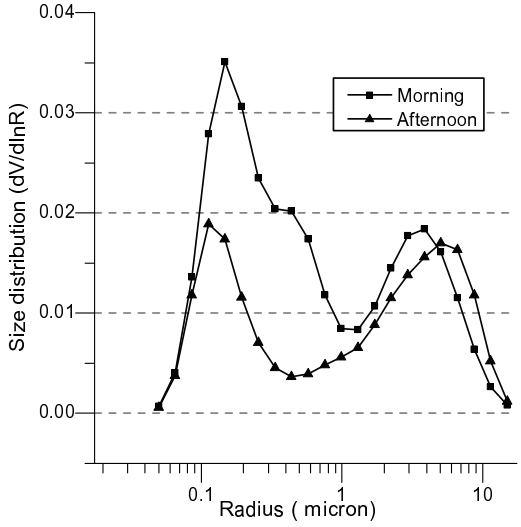

Fig. 2. Size distribution of aerosol at the moment of plane transit over TF on 10 August 2012.

calculated from the AOTs at 665 and 865 nm as follows:

$$\alpha = -\frac{\log(\tau_1/\tau_2)}{\log(\lambda_1/\lambda_2)}, \tag{8}$$

where λ_1 and λ_2 are two wavelengths, τ_1 and τ_2 are the relative AOTs of the wavelengths.

The polarized phase function (P) and single scattering albedo (SSA) are calculated using the Mie theory (Bohren and Huffman, 1983; Grainger et al., 2004) by assuming spherical aerosol particles. The LUT structure is summarized in Table 1. The polarized reflectance was calculated using a vector radiative transfer model called successive order of scattering (SOS) (Lenoble et al., 2007). In the AMPR method, the LUT is used to store the aerosol polarized reflectance only, thus the surface polarized reflectance is not included. The simulated polarized reflectance at the instrument level was calculated using Eq. (3).

Figure 3 shows the aerosol retrieval scheme. A least-square fitting method was used to search for the simulated polarized reflectance, $R_{\mathrm{p,simu}}$, that best matches the measured polarized reflectance, $R_{\mathrm{p,meas}}$. The aerosol properties and surface reflectance converge to the actual value. In the condition of M wavelengths and N viewing angles, the residual term

Table 1. Structure of LUT.

Variable	Entries	Number of Entries
Wavelength	665, 865, and 1640 nm	3
AOT	0 : 0.01 : 0.99	100
Ångström exponent	0.1 : 0.1 : 2	20
Solar zenith angle	0° : 1° : 70°	71
View zenith angle	−60° : 1° : 60°	121
Relative azimuth angle	0° : 5° : 180°	37

can be defined as:

$$\Delta = \sum_{i=1}^{M}\sum_{j=1}^{N}[R_{\mathrm{p,simu}}(\lambda_i,\theta_{\mathrm{s}j},\theta_{\mathrm{v}j},\varphi_j,a) - R_{\mathrm{p,meas}}(\lambda_i,\theta_{\mathrm{s}j},\theta_{\mathrm{v}j},\varphi_j,a)]^2, \tag{9}$$

where λ_i is the ith wavelength. $\theta_{\mathrm{s}j}, \theta_{\mathrm{v}j}$ and φ_j are the jth viewing geometry.

The AMPR measured polarized reflectance at 1640 nm was used as the initial estimation of the land surface by assuming that the aerosol and atmospheric molecule scattering were small (Wang et al., 2005). The flow chart (Fig. 3) mechanism can be summarized as follows:

(1) Input the estimation of surface reflectance into the al-

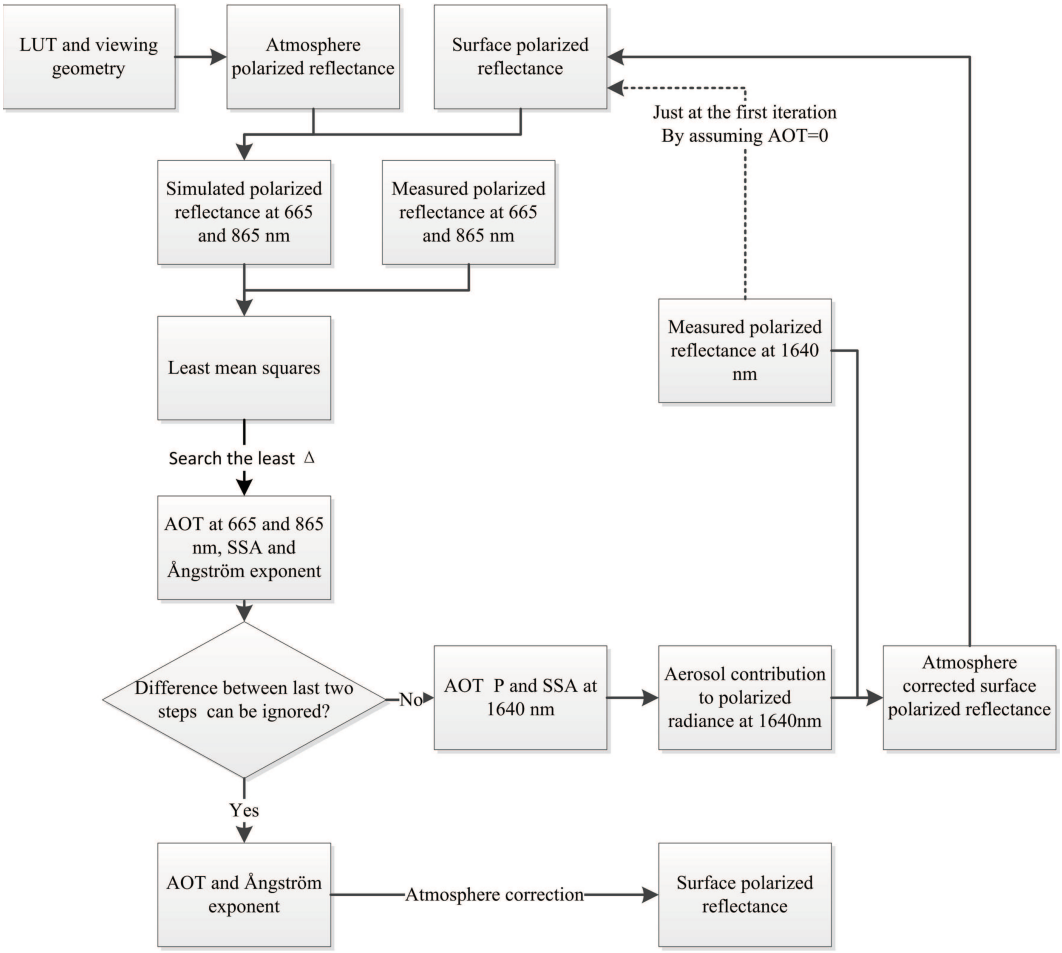

Fig. 3. Flow chart of AMPR retrieval algorithm.

gorithm;

(2) Calculate $R_{\mathrm{p,simu}}$ from the LUT and the surface reflectance using Eq. (3);

(3) Calculate the least residual term using Eq. (9) and search the least one. The aerosol properties at 665 and 865 nm were obtained synchronously;

(4) Can the difference between the last steps be ignored? If no, work through steps 5 to 7. If yes, the aerosol properties have been obtained, so go to step 8;

(5) Estimate the aerosol properties at 1640 nm from the properties at 665 and 865 nm using Eq. (8) and calculate the aerosol polarized reflectance at 1640 nm from the LUT;

(6) Calculate the surface polarized reflectance ($R_{\mathrm{p,surf}}$) by eliminating the aerosol polarized reflectance from the measured polarized reflectance at 1640 nm using the derivative of Eq. (3);

(7) The surface polarized reflectance from step 6 is used as the input of the surface reflectance and start over from steps 1 to 3;

(8) Calculate the surface polarized reflectance ($R_{\mathrm{p,surf}}$) using the derivative of Eq. (3).

3.3. *Surface contribution to upwelling polarized radiance*

The surface polarized reflectance was obtained in step 8. At the same time, the surface polarized model [Eq. (10)], developed by Nadal and Bréon (1999), was used to estimate the surface polarized reflectance for validation:

$$R_{\mathrm{p,surf}}(\theta_{\mathrm{s}},\theta_{\mathrm{v}},\varphi)=\rho\left\{1-\exp\left[-\beta\frac{F_{\mathrm{p}}(\gamma)}{\mu_{\mathrm{s}}+\mu_{\mathrm{v}}}\right]\right\}, \qquad (10)$$

where $\gamma=(\pi-\Theta)/2$ is the incident angle on the reflected element, Θ is the scattering angle, and F_{p} is the Fresnel coefficient for polarized light. ρ and β are empirical coefficients that are determined from the normalized difference vegetation index (NDVI) of the observed surface and the ground-type classification.

The NDVI was computed using the reflectance at 665 and 865 nm. Parameters ρ and β are from Nadal and Bréon (1999). Figure 4 shows the surface polarized reflectance calculated by the two methods. It can be found that the angular responses of surface polarization are at the same current. The differences between these two methods are in the order of magnitude of 10^{-4}, less than 1/10 of the total polarized reflectance. That is to say, an accurate surface polarized reflectance can be obtained from the AMPR algorithm.

4. Experiments

To validate the algorithm and monitor the aerosol distribution over the Beijing–Tianjin–Tangshan region, the AMPR experiment was conducted in Tianjin on 10 August 2012. The area covered east of Tianjin, south of Tangshan, and a corner of Bohai Bay as shown in Fig. 5. A large area of farmland in Tangshan, primarily covered by plants, was chosen as the target field (TF). Haze was present in this area during the morning but disappeared in the afternoon.

Two experimental flights (Y-12 airplane) were performed in the morning and afternoon along the same path. The summaries of the flights are presented in Table 2. In the morning, the AMPR scan direction was along the flight track while it was across the track in the afternoon. The AMPR scan angle was limited to between -38° and $+29^{\circ}$ because of the smaller dimensions of the downward window in the plane. A POS AV (position and attitude recorder made by Applanix Company) was used to record the position and attitude of the AMPR.

Figure 5 shows a map of the local conditions and flight track. The red line is the segment of the flight track. The white square is the TF, which is mainly covered by plants. The ground-based CE318 is situated in Qichang (39.1773°N, 118.3404°W, the white star) south of the TF. It provided the spectral AOT, the aerosol complex refractive index, and par-

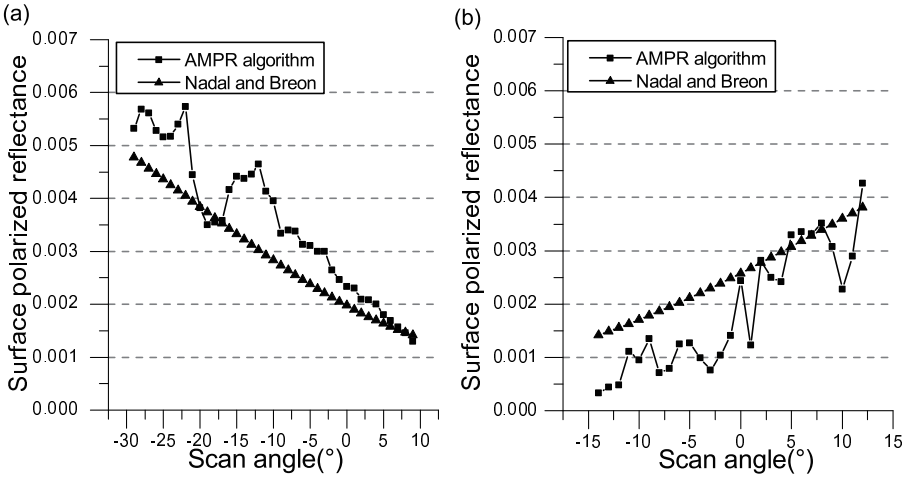

Fig. 4. Surface polarized reflectance over vegetation computed using AMPR algorithm and Nadal and Bréon (NDVI > 0.3, $\rho = 0.007$, and $\beta = 140$) method: (a) solar zenith angle = 32.0°, in the morning; (b) solar zenith angle = 37.2°, in the afternoon.

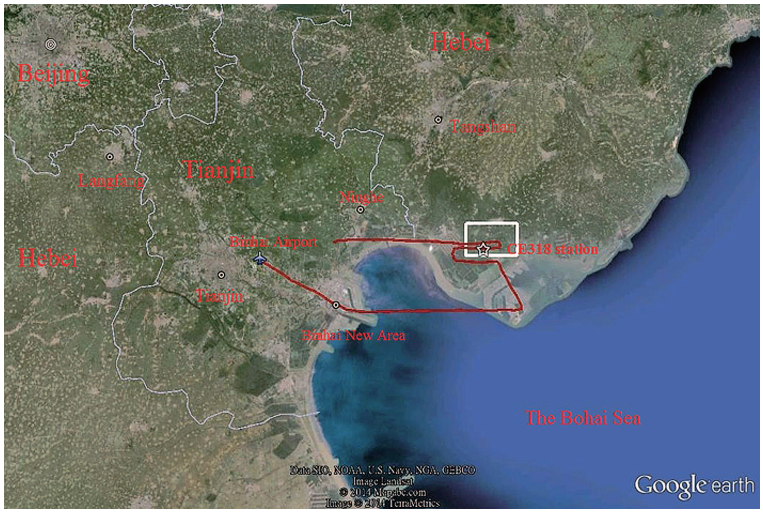

Fig. 5. Map of experimental field and flight track segment in Tianjin experiment.

Table 2. Main characteristics of the flight on 10 August 2012.

	Time (UTC)	Flight area	Altitude	Scan angle	Weather
Morning	0149–0253	117.3°–118.6°E 38.9°–39.21°N	3.1 km	−38° to +29°	Sunny, cloudless
Afternoon	0506–0647	117.3°–118.6°E 38.96°–39.21°N	3.2 km	−38° to +29°	Sunny, cloudless

ticle size distribution.

5. Results

A case study of the AMPR observations performed in the TF is presented. The AOT at 665 nm and the Ångström exponent (computed between AOTs at 665 and 865 nm) were retrieved from the AMPR measurements. The same constraints (AOT at 670 nm and the Ångström exponent, which was computed between AOTs at 670 nm and 870 nm) from the CE318 measurements in the TF were used to validate the AMPR retrievals.

Figure 6 shows the simulated and measured polarized re-

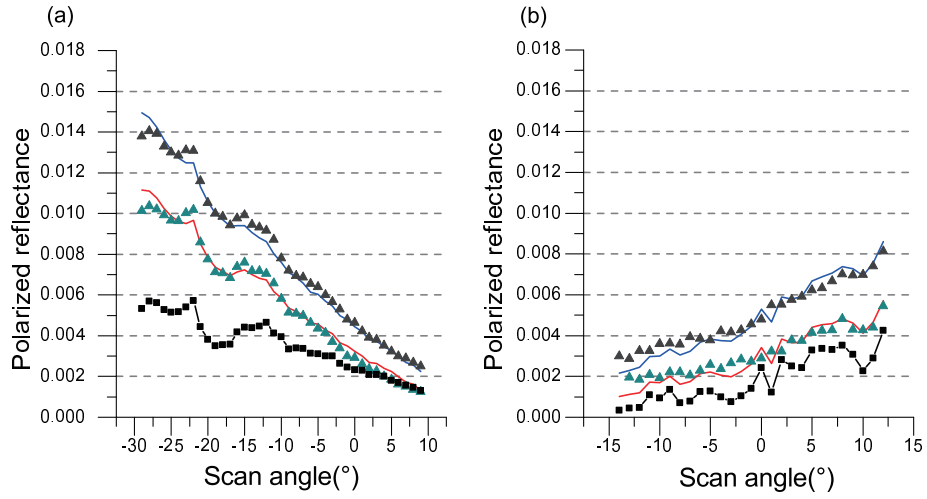

Fig. 6. Simulated, measured and surface polarized reflectance at the aircraft altitude: (a) solar zenith angle = 32.0° in the morning; (b) solar zenith angle = 37.2° in the afternoon. Green (665 nm) and red (865 nm) lines are the simulated polarized reflectance. Dark gray (665 nm) and dark cyan (865 nm) symbols are the measured polarized reflectance. Black line and symbols are the surface polarized reflectance.

Table 3. AOT and Ångström exponent retrieved from AMPR and CE318.

	Morning			Afternoon		
Instrument	Time (UTC)	AOT	Ångström exponent	Time (UTC)	AOT	Ångström exponent
CE318	0231	0.243	1.33	0612	0.109	1.61
AMPR	0233	0.21	1.5	0622	0.1	1.7
CE318	0234	0.231	1.35	0633	0.103	1.50

flectance at the height of the aircraft. The atmospheric polarized reflectance was computed using the SOS model with a black surface. The aerosol microphysical properties were derived from the CE318 measurement. The surface polarized reflectance was derived from the AMPR calculation process. The simulated polarized reflectance (atmosphere +surface) was calculated from Eq. (3) and has good agreement with the measurements.

Retrievals of CE318 (before and after the overflight) and AMPR in the morning and afternoon are reported in Table 3. The AMPR retrieved AOT was smaller than the CE318 retrieved AOT while the Ångström exponent was larger. One of the reasons is that polarized light stems mainly from small particles (Deuzé et al., 2001). Another reason may be the overestimation of the land surface albedo by using the reflectance of 1640 nm as the initial estimate of the land surface.

The RSP algorithm was used to verify the AMPR algorithm. Measurements at 1640 nm were substituted for the 2250 nm wavelength retrievals in the RSP algorithm (Fig. 7). Retrievals of CE318 at the moment of the plane transit were used to verify the results. On the whole, the retrievals of both the algorithms were consistent and close to the retrievals of CE318.

Aerosols over the TF appear to be a mixture of different types (e.g., urban-industrial and oceanic). The fine mode, urban-industrial aerosols correspond to large Ångström exponent values, while the coarse mode marine aerosols correspond to smaller Ångström exponent values. The marine aerosols and morning haze were dominant during the morn-

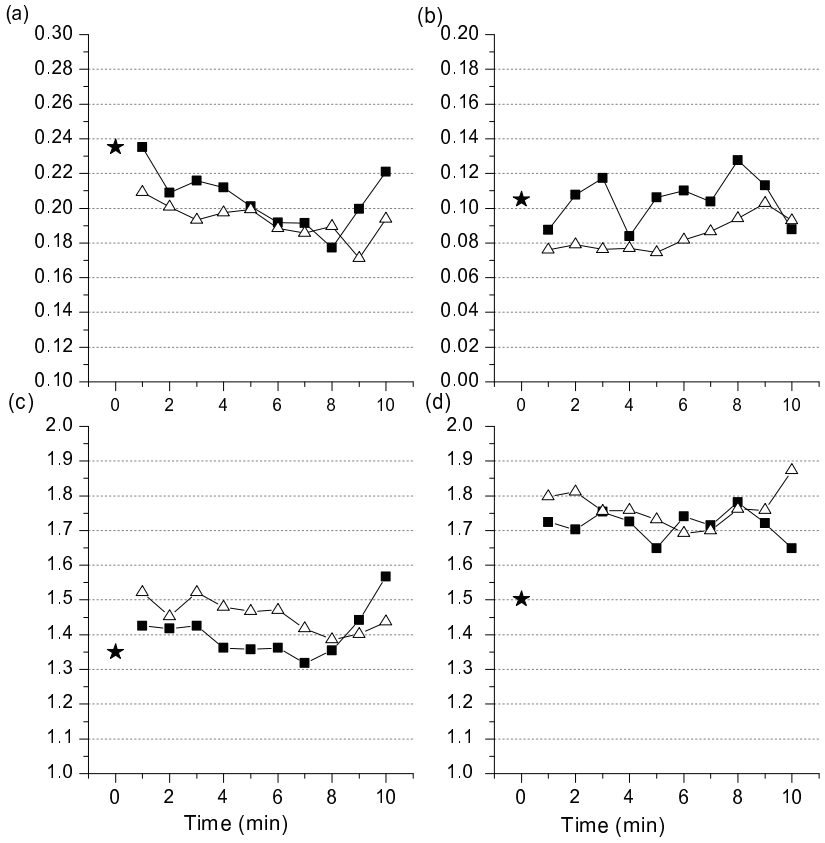

Fig. 7. Retrieved AOT and Ångström exponent over TF from the AMPR algorithm (line and squares), RSP algorithm (line and triangles), and CE318 (the black star). (a) AOT in the morning; (b) AOT in the afternoon; (c) Ångström exponent in the morning; and (d) Ångström exponent in the afternoon. Time = 0 is the CE318 results. Time = 1 is 0827 LST in the morning and 1418 LST in the afternoon.

ing hours, but in the afternoon the dominant mode shifted to the urban-industrial aerosols. The AOT became smaller as the morning haze disappeared. These results suggest a diurnal cycle in aerosol variability.

6. Conclusions

The AMPR is a newly developed instrument. It provides directional, polarized, and multi-spectral measurements. We developed an algorithm to retrieve the aerosol optical thickness and the Ångström exponent based on the AMPR measurements. The algorithm is based on a LUT and an iterative method. Experiments in Tianjin were conducted to validate the algorithm.

Using the aerosol retrieval algorithm for the AMPR measurement, the temporal variability of the aerosol optical properties over the TF were analyzed. The results in the morning and afternoon were analyzed and compared with CE318 measurements. Agreement between the retrievals of the AMPR and the nearby CE318 is adequate. Along the flight line, the retrievals of the AMPR algorithm match the retrievals of the RSP algorithm and CE318 well, which demonstrates the potential of the AMPR algorithm. The preliminary validation is encouraging.

However, limited cases make further comparisons difficult. More experiments (currently in progress) will yield future valid results as new equipment designed to obtain the surface bidirectional polarization distribution function (BPDF) of land surfaces is being developed. The degree of overestimation of land surface properties when using the AMPR can be reduced by using this equipment. Combining this new approach with LIDAR will enhance the ability of the AMPR to quantify particle size and will also be addressed in future studies.

Acknowledgements. This research was supported by the Chinese Airborne Remote Sensing System, the Major National Science and Technology Infrastructure Construction Projects, and the Key Programs of the Chinese Academy of Sciences (Grant No. KGFZD-125-13-006). The authors are grateful for the helpful suggestions of researcher LI Zhengqiang and his team from the Institute of Remote Sensing Applications.

REFERENCES

Bréon, F. M., J. L. Deuzé, D. Tanré, and M. Herman, 1997: Validation of spaceborne estimates of aerosol loading from Sun photometer measurements with emphasis on polarization. *J. Geophys. Res.*, **102**, 17 187–17 195.

Brunekreef, B., and S. T. Holgate, 2002: Air pollution and health. *The Lancet*, **360**(9341), 1233–1242.

Bohren, C. F., and D. R. Huffman, 1983: *Absorption and Scattering of Light by Small Particles*. John Wiley, New York, 448 pp.

Cairns, B., L. D. Travis, and E. E. Russell, 1997: Polarization: Ground-based upward-looking and aircraft/satellite-based downward-looking measurements. *Proc. SPIE*, Vol. 3220, Satellite Remote Sensing of Clouds and the Atmosphere II, 103 (January 1, 1997), doi: 10.1117/12.301140.

Cairns, B., B. E. Carlson, R. X. Ying, A. A. Lacis, and V. Oinas, 2003: Atmospheric correction and its application to an analysis of Hyperion data. *IEEE Trans. Geosci. Remote Sens.*, **41**(6), 1232–1245.

Cheng, T. H., X. F. Gu, D. H. Xie, Z. Q. Li, T. Yu, and X. F. Chen, 2011: Simultaneous retrieval of aerosol optical properties over the Pearl River Delta, China using multi-angular, multi-spectral, and polarized measurements. *Remote Sens. Environ.*, **115**, 1643–1652.

Chowdhary, J., B. Cairns, and L. Travis, 2002: Case studies of aerosol retrievals over the ocean from multiangle, multispectral photopolarimetric remote sensing data. *J. Atmos. Sci.*, **59**(3), 383–397.

Chowdhary, J., and Coauthors, 2005: Retrieval of aerosol scattering and absorption properties from photopolarimetric observations over the ocean during the CLAMS experiment. *J. Atmos. Sci.*, **62**, 1093–1117, doi: 10.1175/JAS3389.1.

Dai, T., D. Goto, N. A. J. Schutgens, X. Dong, G. Shi, and T. Nakajima, 2014: Simulated aerosol key optical properties over global scale using an aerosol transport model coupled with a new type of dynamic core. *Atmos. Environ.*, **82**, 71–82.

Deuzé, J. L., F. M. Bréon, P. Y. Deschamps, C. Devaux, M. Herman, A. Podaire, and J. L. Roujean, 1993: Analysis of POLDER (POLarization and Directionality of Earth's Reflectances) airborne instrument observations over land surfaces. *Remote Sens. Environ.*, **45**, 137–154.

Deuzé, J. L., and Coauthors, 2001: Remote sensing of aerosols over land surfaces from POLDER-ADEOS-1 polarized measurements. *J. Geophys. Res.*, **106**, 4913–4926.

Diner, D. J., J. V. Martonchik, R. A. Kahn, B. Pinty, N. Gobron, D. L. Nelson, and B. N. Holben, 2005: Using angular and spectral shape similarity constraints to improve MISR aerosol and surface retrievals over land. *Remote Sens. Environ.*, **94**, 155–171.

Duan, A. M., G. X. Wu, Y. M. Liu, Y. M. Ma, and P. Zhao, 2012: Weather and climate effects of the Tibetan Plateau. *Adv. Atmos. Sci.*, **29**(5), 978–992, doi: 10.1007/s00376-012-1220-y.

Dubovik, O., and M. D. King, 2000: A flexible inversion algorithm for retrieval of aerosol optical properties from Sun and sky radiance measurements. *J. Geophys. Res.*, **105**, 20 673–20 696.

Dubovik, O., and Coauthors, 2011: Statistically optimized inversion algorithm for enhanced retrieval of aerosol properties from spectral multi-angle polarimetric satellite observations. *Atmospheric Measurement Techniques Discussions*, **3**, 4967–5077.

Grainger, R. G., J. Lucas, G. E. Thomas, and G. B. Ewen, 2004: Calculation of Mie derivatives. *Appl. Opt.*, **43**, 5386–5393.

Hansen, J. E., M. Sato, A. Lacis, R. Ruedy, I. Tegen, and E. Matthews, 1998: Climate forcings in the industrial era. *Proceedings of the National Academy of Sciences of the United States of America*, **95**, 12 753–12 758.

Hasekamp, O., P. Litvinov, and B. André, 2011: Aerosol properties over the ocean from PARASOL multiangle photopolarimetric measurements. *J. Geophys. Res.*, **116**, D14204, doi: 10.1029/2010JD015469.

Hauser, A., D. Oesch, N. Foppa, and S. Wunderle, 2005: NOAA AVHRR derived aerosol optical depth over land. *J. Geophys. Res.*, **110**, D08204. doi: 10.1029/2004JD005439.

Haywood, J. and O. Boucher, 2000: Estimates of the direct and indirect radiative forcing due to tropospheric aerosols: a review.

Rev. Geophys., **38**, 513–544.

Knobelspiesse, K. D., B. Cairns, B. Schmid, M. O. Román, and C. B. Schaaf, 2008: Surface BRDF estimation from an aircraft compared to MODIS and ground estimates at the Southern Great Plains site. *J. Geophys. Res.*, **113**, D20105, doi: 10.1029/2008JD010062.

Lafrance, B., 1997: Simplified model of the polarized light emerging from the atmosphere. Correction of the stratospheric aerosol impact on POLDER measurements. Ph. D. dissertation, Université des Sciences et Techniques de Lille, France. (in French)

Lenoble, J., M. Herman, J. L. Deuzé, B. Lafrance, R. Santer, and D. Tanré, 2007: A successive order of scattering code for solving the vector equation of transfer in the earth's atmosphere with aerosols. *Journal of Quantitative Spectroscopy and Radiative Transfer*, **107**(3), 479–507.

Li, Z. Q, P. Golouba, C. Devaux, X. F. Gu, J. L. Deuzé, Y. L. Qiao, and F. S. Zhao, 2006: Retrieval of aerosol optical and physical properties from ground-based spectral, multi-angular, and polarized sun-photometer measurements. *Remote Sens. Environ.*, **101**(4), 519–533.

Mishchenko, M. I., and L. D. Travis, 1997: Satellite retrieval of aerosol properties over the ocean using polarization as well as intensity of reflected sunlight. *J. Geophys. Res.*, **102**, 16 989–17 013.

Nadal, F., and F. M. Bréon, 1999: Parameterization of surface polarized reflectance derived from POLDER spaceborne measurements. *IEEE Trans. Geosci. Remote Sens.*, **37**, 1709–1718.

Remer, L. A., and Coauthors, 2005: The MODIS aerosol algorithm, products, and validation. *J. Atmos. Sci.*, **62**(4), 947–973.

Song, M. X., B. Sun, X. B. Sun, and J. Hong, 2012: Polarization calibration of airborne multi-angle polarimetric radiometer. *Optics and Precision Engineering*, **20**(6), 1153–1158. (in Chinese)

Wang, X. H., J. Hong, Y. L. Qiao, F. G. Meng, Y. J. Zhang, and P. Gong, 2005: Retrieval of aerosol optical thickness with dual-angle multispectral means. *High Technology Letters*, **15**(9), 101–105. (in Chinese)

Waquet, F., J. F. Léon, P. Goloub, J. Pelon, D. Tanré, and J. L. Deuzé, 2005: Maritime and dust aerosol retrieval from polarized and multispectral active and passive sensors. *J. Geophys. Res.*, **110**, D10S10, doi: 10.1029/2004JD004839.

Waquet, F., P. Goloub, J. L. Deuzé, J. F. Léon, F. Auriol, C. Verwaerde, J. Y. Balois, and P. François, 2007: Aerosol retrieval over land using a multiband polarimeter and comparison with path radiance method. *J. Geophys. Res*, **112**, D11214, doi: 10.1029/2006JD008029.

Waquet, F., B. Cairns, K. Knobelspiesse, J. Chowdhary, L. D. Travis, B. Schmid, and M. I. Mishchenko, 2009a: Polarimetric remote sensing of aerosols over land. *J. Geophys. Res.*, **114**, D01206, doi: 10.1029/2008JD010619.

Waquet, F., J. F. Léon, B. Cairns, P. Goloub, J. L. Deuzé, and F. Auriol, 2009b: Analysis of the spectral and angular response of the vegetated surface polarization for the purpose of aerosol remote sensing over land. *Appl. Opt.*, **48**(6), 1228–1236.